Nucleic Acids Research, 2014, Vol. 42, No. 15 **10099–10111**
doi: 10.1093/nar/gku686

NAR Breakthrough Article

7SL RNA represses p53 translation by competing with HuR

Kotb Abdelmohsen*, Amaresh C. Panda, Min-Ju Kang, Rong Guo, Jiyoung Kim, Ioannis Grammatikakis, Je-Hyun Yoon, Dawood B. Dudekula, Ji Heon Noh, Xiaoling Yang, Jennifer L. Martindale and Myriam Gorospe*

Laboratory of Genetics, National Institute on Aging, National Institutes of Health, Baltimore, MD 21224, USA

Received April 11, 2014; Revised July 13, 2014; Accepted July 16, 2014

ABSTRACT

Noncoding RNAs (ncRNAs) and RNA-binding proteins are potent post-transcriptional regulators of gene expression. The ncRNA *7SL* is upregulated in cancer cells, but its impact upon the phenotype of cancer cells is unknown. Here, we present evidence that *7SL* forms a partial hybrid with the 3′-untranslated region (UTR) of *TP53* mRNA, which encodes the tumor suppressor p53. The interaction of *7SL* with *TP53* mRNA reduced p53 translation, as determined by analyzing p53 expression levels, nascent p53 translation and *TP53* mRNA association with polysomes. Silencing *7SL* led to increased binding of HuR to *TP53* mRNA, an interaction that led to the promotion of p53 translation and increased p53 abundance. We propose that the competition between *7SL* and HuR for binding to *TP53* 3′UTR contributes to determining the magnitude of p53 translation, in turn affecting p53 levels and the growth-suppressive function of p53. Our findings suggest that targeting *7SL* may be effective in the treatment of cancers with reduced p53 levels.

INTRODUCTION

Long noncoding RNAs (lncRNAs; >200 nucleotides) have emerged as potent regulators of gene expression at different levels, including chromatin remodeling, transcriptional and post-transcriptional control and protein metabolism (1,2). At the post-transcriptional level, lncRNAs can modulate mRNA decay and translation working jointly with microRNAs (miRNAs) and with RNA-binding proteins (RBPs) such as HuR and Staufen 1 [reviewed in (2)]. For instance, the lncRNAs *1/2-sbsRNAs* (1/2-Staufen 1-binding site) interact with target mRNAs containing Alu elements in the 3′ untranslated region (UTR) by imperfect base-pairing and recruitment of the RBP Staufen 1 to promote decay (3). In contrast, the lncRNA *BACE1AS* (β amyloid-cleaving enzyme 1 antisense) forms a region of perfect base-pairing with *BACE1* mRNA, which encodes an enzyme involved in cleaving the protein APP (amyloid precursor protein), and protects *BACE1* mRNA from RNase-mediated degradation (4); this effect was attributed, at least in part, to the fact that the region of complementarity prevents binding of miR-485-5p to the *BACE1* 3′UTR (5). Examples of the impact of lncRNAs on mRNA translation have also been reported. For example, *Uchl1* mRNA (encoding ubiquitin carboxyterminal hydrolase) was recently found to interact with antisense (AS) *Uchl1 lncRNA* via short interspersed element (SINE) sequences, leading to enhanced mRNA translation (6). Among the lncRNAs that inhibit translation, *lincRNA-p21* repressed the translation of *JUNB* and *CTNNB* mRNAs by forming partial hybrids and recruiting translation repressors Rck and Fmrp (7).

RBPs are broadly involved in regulating gene expression at all post-transcriptional levels, including pre-mRNA splicing, transport, stability and translation (8–10). The RBP HuR has three RNA recognition motifs through which it binds numerous mRNAs to enhance their translation or stability, as well as many pre-mRNAs and noncoding RNAs (both miRNAs and lncRNAs) (7,11). Through its impact on target RNAs, HuR has been implicated in several cellular processes, including cell division, survival, senescence, immune activation and the stress response, as well as in pathological conditions such as cancer (12,13).

HuR function is regulated by three major mechanisms. HuR abundance is negatively regulated by miRNAs (miR-519, miR-125), ubiquitination and caspase-mediated cleav-

---

*To whom correspondence should be addressed. Tel: +1 410 558 8589; Fax: +1 410 558 8331; Email: abdelmohsenk@mail.nih.gov
Correspondence may also be addressed to Myriam Gorospe. Tel: +1 410 558 8443; Fax: +1 410 558 8331; Email: myriam-gorospe@nih.gov

Published by Oxford University Press on behalf of Nucleic Acids Research 2014.

age in response to apoptotic stress [reviewed in (13)]. HuR subcellular localization is governed via phosphorylation by Cdk1, PKC and JAK3, and via methylation (13–15). HuR binding to mRNAs is controlled through phosphorylation by Chk2, PKC and JAK3 (13–15), and is competed by other RBPs (e.g. AUF1) or by miRNAs (e.g. miR-122, miR-494) (16–18). However, whether lncRNAs modulate HuR function is unknown.

The 300-nt long ncRNA *7SL* (NR_002715; gene name *RN7SL1*) forms a ribonucleoprotein complex (RNP) with six signal-recognition proteins (SRPs). The RNP binds signal sequences of secretory and transmembrane proteins to facilitate their targeting to the membrane translocation apparatus in the endoplasmic reticulum (19,20). Chen *et al.* previously reported increased expression of the BC200 (related to *7SL*) in cancer cells [(21), reviewed by White (22)], but the impact of this enhanced expression on cancer cell fate is not known. Here, we report that *7SL* is highly expressed in cancer tissues and its silencing resulted in a significant reduction in cell proliferation. We identified an interaction between *7SL* and the 3′UTR of *TP53* mRNA, encoding the tumor suppressor p53, that led to the suppression of p53 translation. HuR also binds the *TP53* 3′UTR and promotes p53 translation, but binds immediately outside of the *7SL* binding sites (9,23). Interestingly, *7SL* silencing led to increased HuR binding to *TP53* mRNA and promoted p53 translation and p53 accumulation, indicating that *7SL* functionally prevented HuR binding to *TP53* mRNA and suggesting that *7SL* and HuR might compete for binding *TP53* mRNA. We further discovered that *7SL* promotes cancer cell growth by repressing p53 production, as p53-deficient cells were refractory to the growth-inhibitory effects of silencing *7SL*. The enhanced expression of p53 in *7SL*-silenced cells promoted cell cycle arrest, senescence and autophagy. We conclude that the proliferative effects of the ncRNA *7SL* are mediated in part by displacement of HuR from *TP53* mRNA leading to repression of p53 translation and p53 accumulation in cancer cells.

MATERIALS AND METHODS

Tumor and normal tissues, and cell culture, transfection and proliferation

Total RNAs from normal and adjacent cancer tissues were purchased from BioChain Institute, Inc. (liver, lung, breast, stomach) or obtained from the University of Maryland Tissue Bank samples (kidney, ovary, breast). Human cervical carcinoma HeLa cells and human pancreatic adenocarcinoma MiaPaCa cells were cultured in Dulbecco's modified Eagle's medium containing 5% fetal bovine serum (FBS), human colorectal carcinoma RKO cells in minimum essential medium (+10% FBS), and colon cancer HCT116 cells were in McCoy's 5A (+10% FBS). All cultures were supplemented with antibiotics. Transfection of cells (∼50% confluence) was carried out using lipofectamine 2000 (Invitrogen). The siRNAs used (from Qiagen) were Ctrl siRNA (AATTCTCCGAACGTGTCACGT), HuR siRNAs (AAACCAACAAGTCCCACAAAT, AATCTTAAGTTTCGTAAGTTA and TTCCTTTAAGATATATATTAA) and 7SL siRNA (AAGCACTAAGTTCGGCATCAA); SRP proteins were silenced using siRNAs from Santa Cruz Biotechnology directed to SRP68 [sc-94109], SRP19 [sc-44117] and SRP54 [sc-106810].

Plasmid pcDNA3-7SL was prepared by cloning polymerase chain reaction (PCR)-amplified *7SL*. Luciferase reporter constructs were pmirGlo (control), pmirGlo-p53 (3′UTR) and pmirGlo-p53 (3′UTRΔ), the latter lacking 140 nt (2161–2300) and thus missing the region of interaction with *7SL*. Forty-eight hours after siRNA transfection, DNA replication was assessed by measuring [^{3}H]-thymidine incorporation, and cell cycle distribution was assessed using propidium iodide-stained, ethanol-fixed cells (analyzed using Multicycle software) as described (24). To assay luciferase reporter activity, cells were lysed and firefly and Renilla luciferase activities were measured using Dual-Luciferase Assay system (Promega) and a 96-well Microplate Luminometer BD Pharmingen™ Monolight 3096. The ratios of firefly luciferase (FL) to Renilla luciferase (RL) activities were determined, and all values were normalized to those of control cells, transfected with an empty vector.

Protein analysis

Whole-cell lysates were prepared using radioimmunoprecipitation assay (RIPA) buffer, resolved by sodium dodecyl sulphate-polyacrylamide gel electrophoresis (SDS-PAGE) and transferred onto polyvinylidene difluoride (PVDF) membranes. After incubations with primary mouse monoclonal antibodies recognizing HuR, p53, β-tubulin, p21, SRP68, SRP54, HSP90 (all Santa Cruz Biotechnology), LC3-II (Abcam) and β-actin (Abcam), blots were incubated with the appropriate secondary antibodies (Amersham) and signals detected using enhanced luminescence (Amersham).

Nascent (*de novo*) translation of p53 and β-tubulin was studied as described (24). Briefly, HeLa cells were incubated with 1 mCi L-[^{35}S]methionine and L-[^{35}S]cysteine (Easy Tag ™EXPRESS, NEN/Perkin Elmer) per 60-mm plate for 15 min. Cells were lysed in RIPA buffer [10 mM Tris-HCl (pH 7.4), 150 mM NaCl, 1% Nonidet P-40, 1 mM EDTA, 0.1% SDS and 1 mM DTT] and immunoprecipitation (IP) reactions carried out in TNN buffer [50 mM Tris-HCl (pH 7.5), 250 mM NaCl, 5 mM EDTA, 0.5% Nonidet P-40] for 16 h at 4°C using anti-IgG1 (BD PharMingen), anti-β-tubulin and anti-p53 antibodies. Following extensive washes in TNN buffer, the IP samples were resolved by SDS/PAGE, transferred onto PVDF filters and visualized with a PhosphorImager (Molecular Dynamics).

RNA analysis

Total cellular RNA was prepared using TRIzol (Invitrogen) or was isolated after RIP analysis [IP of cellular RNP (ribonucleoprotein) complexes using anti-HuR or IgG as described (25). After reverse transcription (RT) using random hexamers and Maxima reverse transcriptase (Fermentas), quantitative PCR (qPCR) analysis was performed using gene-specific primer pairs and SYBR Green PCR master mix (Kapa Biosystems). Specific forward and reverse primers to detect endogenous RNAs using RT-qPCR analysis were: CAAAACTCCCGTGCTGATCA and GGCTGGAGTGCAGTGGCTAT for

7SL, ATGGAAATCCCATCACCATCTT and CGCCCCACTTGATTTTGG for *GAPDH*, GAAGGAAATGGCCAAACAGA and ACGCTTTCTCCAGGTCTTCA for *NCL*, CAGGTTGCGGGAATCCAAAG and GCTGGGCACCTAGGACATCG for *SIRT1*, AGAAGGTGGTGGCATTTTTG and CAGTCTTCCCAAAGCAGGAG for *VHL*, AGGCCTTGGAACTCAAGGAT and TGAGTCAGGCCCTTCTGTCT for *TP53*, TCCTGAAACTCCTCTTTGTTTAACTG and CACCAACTCTCCCACTAGGCTATAA for *MIAT*, TGGCAAAATTGAACCAACAA and TTGAATCCCATCATGCCTTT for *SRP54*, CAGGCAGCTACCATGAGTGA and TCAAACAGGCGCTCCTTAGT for *SRP68*, and GAAGGCGAATCCCCATAAGT and CCGGACTCTGCCTCTGTATT for *SRP19*.

Antisense oligonucleotides (ASOs), biotinylated at the 3′ end, were as follows: AATTCTCCGAACGTGTCACGT (Ctrl-biot-ASO); TTTCACAGATATGGGCCTTGAAGTTAG and AGATGAAATCCTCCAGGGTGTGGGA (TP53-biot-ASO); CACCAACTCTCCCACTAGGCTATAA (MIAT-biot-ASO); GGGTGTGTAGAAGAAGCCACGCTCCCC and TTGCAGTAGTTCTCCAGCTGGTAGAG (INS-biot-ASO), and TGTTTGATGGATAGTTCATGTCTGT and TGAAACATTTCCAAAGCATTTATTT (SIRT1-biot-ASO). RNA and protein in sucrose and glycerol gradients were analyzed as described (24).

Northern blot analysis was performed using standard methods; *7SL* and *18S* were detected after end-labeling the oligonucleotides GTGATTCAAGCCGTAGTTATACCACTGGAG and CCAATGGATCCTCGTTAAAGGATTT, respectively (25).

Sucrose and glycerol gradient analysis

For the analysis of sucrose gradients, HeLa cells were incubated with cycloheximide (Calbiochem; 100 μg/ml, 15 min), and cytoplasmic lysates (500 μl) were prepared in polysome extraction buffer (PEB), fractionated by centrifugation through 10–50% linear sucrose gradients and divided into 10 fractions for RT-qPCR analysis, as described (24).

For glycerol gradient analysis, HeLa cells were lysed in a buffer containing 20 mM Tris-HCl, pH 7.5, 100 mM KCl, 5 mM $MgCl_2$, 0.5% (v/v) Nonidet P-40, RNAse-OUT and 1X protease inhibitor cocktail. After centrifugation (39 000 rpm, 18 h, 4°C) of the lysates through glycerol gradients (10–40%), 12 fractions (1 ml each) were collected; 0.3 ml was used for preparing RNA using TRIzol (Invitrogen) followed by RT-qPCR to measure *7SL* and *18S* rRNA levels, and 0.7 ml was precipitated using trichloroacetic acid (TCA) and used for western blot analysis to detect SRP proteins.

Pulldown of endogenous and biotinylated RNA

HeLa cells were lysed with PEB containing protease inhibitors (Roche) and RNase inhibitor (Thermo Fisher). Lysates were incubated with 100 pmoles of biotin-labeled oligomers complementary to *TP53* mRNA (TP53-biot-ASO) or *MIAT* (MIAT-biot-ASO) for 30 min at RT as described (7). Dynabeads M-280 Streptavidin (Invitrogen) (100 μl) were added and further incubated (1 h, 4°C with rotation). Beads were washed with NT2 buffer, RNA was isolated using TRIzol, and the enrichment of *TP53*mRNA and *7SL* bound to biotinylated ASOs was measured by RT-qPCR.

Biotinylated and non-biotinylated RNA was prepared as explained below. To assess binding of *7SL* to the *TP53* 3′UTR, 25 ng of non-biotinylated *7SL* was incubated with biot-*TP53*(*3*′) or with biot-*TP53*(*3*′*Δ*) (30 min, 37°C) in 1X TENT buffer (10 mM Tris-HCl [pH 8.0], 1 mM EDTA [pH 8.0], 250 mM NaCl, 0.5% [v/v] Triton X-100), and protease and RNase inhibitors. After incubation with Dynabeads M-280 Streptavidin (30 min, 25°C), the beads were washed with phosphate buffered saline (PBS), the RNA isolated using TRIzol, and *7SL* levels in the beads analyzed using RT-qPCR.

To measure HuR binding to *TP53*(*3*′) and *TP53*(*3*′*Δ*), the biotinylated RNAs (25 ng) were incubated for 30 min at 37°C in 1X TENT buffer with protease and RNase inhibitors, in the presence of 0.5 μg GST or GST-HuR. In competition experiments, unlabeled *7SL* or *GAPDH*RNAs (25 ng each) was incubated along with biot-*TP53*(*3*′) and GST-HuR. After incubation with streptavidin dynabeads (30 min, 25°C) and washes with PBS, western blot analysis was used to detect GST-HuR.

Longer biotinylated RNAs were prepared *in vitro* using T7 and using primers (forward and reverse in each case; lowercase letters representing the T7 RNA polymerase promoter sequence): ttctaatacgactcactatagggCTTGTTTTATGCTCAGGGTC and CACCCCTCAGACACACAGGTGGCA for *TP53* 3′UTR, and ttctaatacgactcactatagggGCCGGGCGCGGTGGCGCGTG and AGAGACGGGGTCTCGCTATGTTG for *7SL*.

RESULTS

7SL is selectively elevated in cancer tissues and is required for cell growth

The ncRNA *7SL*, as well as the related ncRNA *BC200*, were shown to be widely upregulated in various cancer types (21,22). In agreement with this finding, RT followed by real-time qPCR analysis revealed higher *7SL* levels in various tumor (T) tissues (liver, lung, breast, stomach) than in normal (N) adjacent tissues (Figure 1A; similar results were obtained by northern blot analysis of other N and T pairs, Supplementary Figure S1). To study the impact of *7SL* on cancer cells, we tested the effect of knocking down *7SL* levels in different cancer cell lines. As shown (Figure 1B), 48 h after transfecting HeLa cells (cervical carcinoma) with 7SL siRNA, *7SL* levels were reduced by ∼60% compared to control cells. Silencing *7SL* significantly reduced cell number in a variety of cultured cancer cell types, including HeLa cells, pancreatic carcinoma (Mia PaCa-2) and colon cancer (HCT116 and RKO) cell lines, and repressed HeLa cell growth (Figure 1C and D). Together, these data indicate that *7SL* is highly expressed in cancer cells and enhanced cancer cell growth.

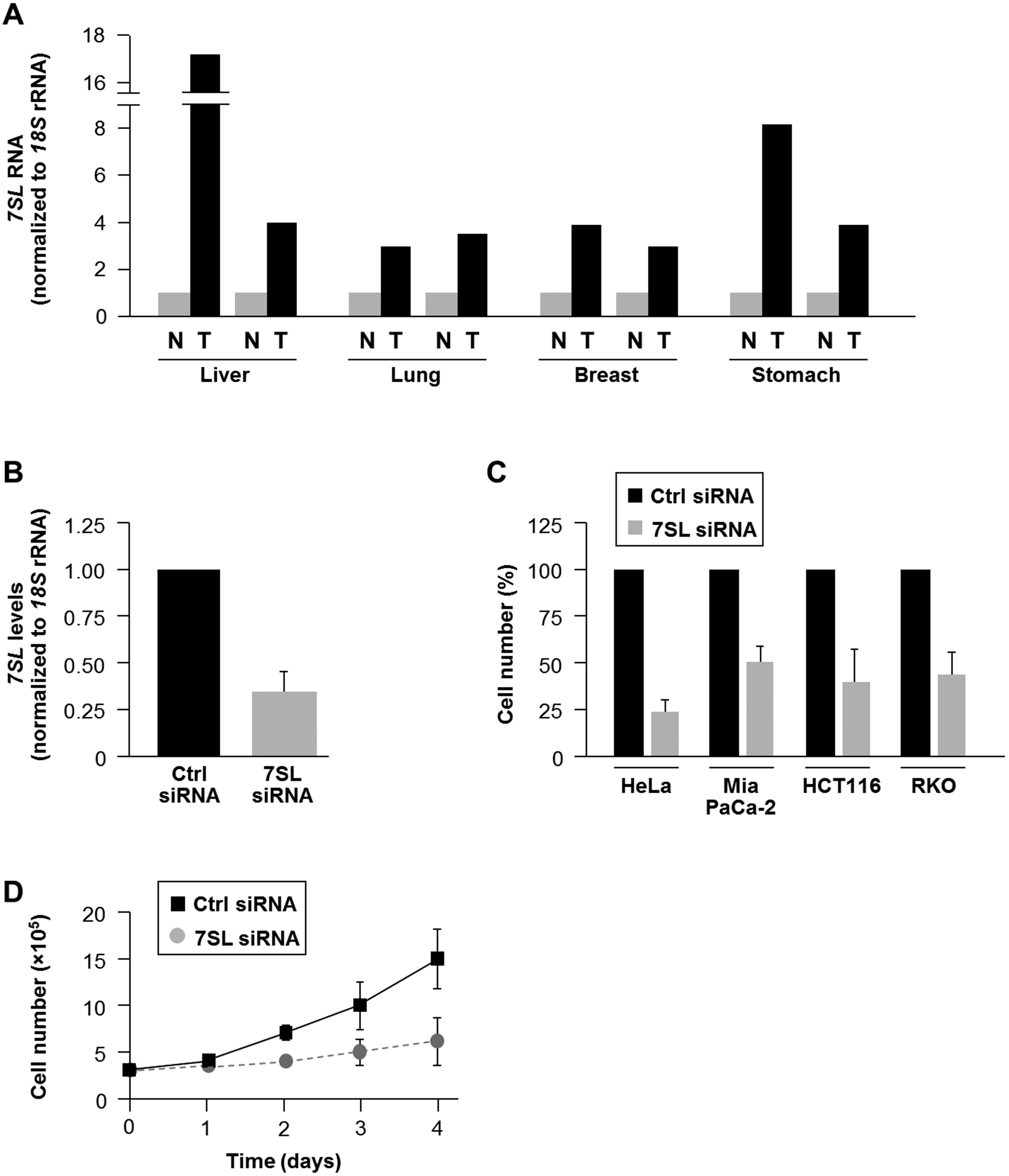

Figure 1. *7SL* is highly expressed in cancer tissues and is required for cell growth. (**A**) The abundance of *7SL* in the tumor tissues (T) indicated (liver, lung, breast, stomach) and adjacent normal tissues (N) was measured by RT-qPCR analysis and normalized to *18S* rRNA levels. (**B**) RT-qPCR analysis of *7SL* levels 48 h after transfection of HeLa cells with Ctrl siRNA or 7SL siRNA. (**C**) Forty-eight hours after siRNA transfection of HeLa, Mia PaCa-2, HCT116 or RKO cells, cell numbers were measured using a hemocytometer and represented as % of cells relative to the Ctrl group. (**D**) Growth kinetics of HeLa cells transfected with Ctrl siRNA or 7SL siRNA. Cells were counted daily for 4 days. Data in (B)–(D) are the means ± S.D. from three independent experiments.

7SL interacts with *TP53* mRNA and lowers p53 abundance

Long ncRNAs can enhance or suppress gene expression by interacting directly with mRNAs (2). A BLAST survey to identify possible interactions between *7SL* and regulators of cell growth revealed that *7SL* was predicted to form extensive regions of sense–antisense interaction with the 3′UTR of the *TP53* mRNA (nucleotides 2209–2367; Figure 2A, Supplementary Figure S2); sequence identities were 85–93%. Other putative interaction partners of *7SL* are listed (Supplementary Table S1). To verify if endogenous *7SL* and *TP53* mRNAs formed hybrid RNA interactions, we designed biotinylated AS oligomers complementary to *TP53* mRNA (TP53-biot-ASO), to a negative control (the lncRNA *MIAT*, MIAT-biot-ASO), and to mRNAs encoding insulin (INS-biot-ASO) and Sirtuin-1 (SIRT1-biot-ASO). Incubation of lysates prepared from HeLa cells with biot-ASOs revealed that *7SL* was enriched in TP53-biot-ASO pulldown samples, but not in the other biot-ASO pulldowns, indicating that *7SL* selectively associated with *TP53* mRNA (Figure 2B). The enrichment of *GAPDH* mRNA in the pulldown samples was measured to assess background RNA binding to biot-ASOs.

Next we asked if *7SL* could influence p53 expression. By 48 h after transfection, silencing *7SL* elevated p53 protein levels in both HeLa and HCT116 cells (Figure 2C) and increased the levels of p21 protein and *CDKN1A* mRNA [encoding p21 (Figure 2C and D), a transcriptional target of p53 (26)], but it did not increase *TP53* mRNA levels (Figure 2D). The increase in p53 expression was not likely due to cell toxicity derived from lowering *7SL* (Supplementary Figure S3). Strong overexpression of *7SL* could not be attained in HeLa cells, but a moderate increase in *7SL* from a plasmid vector was tolerated and led to a reduction in p53 protein levels (Figure 2E); despite higher levels of *7SL* in tumor samples (T), *TP53* mRNA abundance did not consistently differ from that in normal samples (Supplementary Figure S1B). Likewise, silencing *7SL* in the cultured tumor lines only affected *TP53* mRNA modestly, but led to a robust increase in p53 protein levels (Supplementary Figure S1C–E).

Since *7SL* is the RNA component of the signal recognition particle (SRP), we studied if the reduction in p53 protein levels was affected by other SRP components. Silencing protein components of the SRP (SRP19, SRP54 or SRP68; Figure 3A) lowered p53 abundance (Figure 3B) but did not affect the levels of *TP53* mRNA (Figure 3B) or *7SL* (Figure 3C). In addition, silencing SRP proteins did not significantly affect cell viability by 48 h after silencing SRP proteins (Figure 3D). These findings suggest that silencing SRP proteins does not recapitulate the increase in p53 elicited by silencing *7SL* in HeLa cells. To test this possibility further, glycerol gradients were studied in order to study if *7SL* is present in fractions devoid of SRP proteins. As shown in Figure 3E–G, SRP54 and SRP68 overlapped substantially with *7SL* (particularly in fractions 5 through 9 of the gradient), but a sizeable amount of *7SL* was found outside of these fractions. In fact, >30% of *7SL* was detected in fractions that did not have SRP54 or SRP68. These results support the notion that a subset of *7SL* exists outside of the SRPs and further indicate that the influence of *7SL* on p53 expression is likely independent of its function as part of the SRP.

In sum, these data indicate that *7SL* interacts with *TP53* mRNA and lowers p53 protein levels. Since *TP53* mRNA levels were not affected, we set out to investigate if *7SL* reduced p53 translation.

7SL and HuR compete for binding to *TP53* mRNA

The RBP HuR binds the 3′UTR of *TP53* mRNA and promotes its translation following irradiation with ultraviolet light (23). Recent HuR PAR-CLIP data revealed that the sites where HuR binds within *TP53* 3′UTR (11) were adjacent to the site of interaction with *7SL* (Figure 4A; yellow, HuR interaction sites; green, putative *7SL* sites). Since HuR enhances p53 abundance, *7SL* lowers it, and both HuR and *7SL* bind *TP53* 3′UTR, we hypothesized that HuR and *7SL* specifically compete for binding to *TP53* mRNA. To test this possibility, we first silenced *7SL* and studied if this intervention affected HuR binding to target mRNAs (15,18,23). As shown, silencing *7SL* selectively enhanced HuR binding to *TP53* mRNA, but not to *VHL*, *SIRT1* or *NCL* mRNAs (Figure 4B).

To gain more direct evidence that *7SL* associated with *TP53* 3′UTR, we transcribed *in vitro* a biotinylated (biot) *TP53* 3′UTR RNA bearing the putative *7SL* RNA complementarity sites [*TP53*(*3′*), 486 nt long], a biot-*TP53* 3′UTR RNA lacking the *7SL* RNA interaction sites [*TP53*(*3′Δ*), 231 nt long], *7SL*, and biot-*7SL*. RNAs biot-*TP53*(*3′*) and biot-*TP53*(*3′Δ*) were incubated with *7SL*; 30 min later, RNA complexes were pulled down using streptavidin beads, extracted, and *7SL* levels were analyzed by RT-qPCR. As shown (Figure 4C), *7SL* was strongly enriched in biot-*TP53*(*3′*) pulldown samples, indicating that the two RNAs interacted; far less *7SL* was found in biot-*TP53*(*3′Δ*) pulldown samples. Other binding sites on *TP53* mRNA may exist in the regions surrounding the mapped hybrid sites on the *TP53* 3′UTR (green regions), since biot-*TP53*(*3′Δ*) shows residual binding to *7SL* above the background levels seen with the non-target control transcript biot-*GAPDH* (Figure 4C). In keeping with the lack of HuR PAR-CLIP tags in *7SL*, only biot-*TP53*(*3′*) (not biot-*7SL*) pulled down GST-HuR, as detected by western blot analysis (Figure 4D).

It was also important to assess directly if HuR binding to *TP53* 3′UTR was influenced by *7SL*. To this end, we incubated biot-*TP53*(*3′*) with GST-HuR in the presence of *7SL* or a control non-target transcript (*GAPDH* RNA), pulled down the complex with streptavidin beads, and measured GST-HuR levels in the complex. As shown (Figure 4E), adding *7SL* reduced the binding of GST-HuR to *TP53*(*3′*), indicating that *7SL* could function as a competitor and reduced GST-HuR interaction with biot-*TP53*(*3′*). Importantly, GST-HuR binding to biot-*TP53*(*3′Δ*), an RNA that binds HuR but lacks the *7SL* complementarity region, was not competed by *7SL* (Figure 4E). Together, these findings indicate that *TP53* 3′UTR can interact with *7SL* in cells and *in vitro*, and that *7SL* competed with HuR for binding to *TP53* 3′UTR via the regions of *7SL* homology with *TP53* 3′UTR.

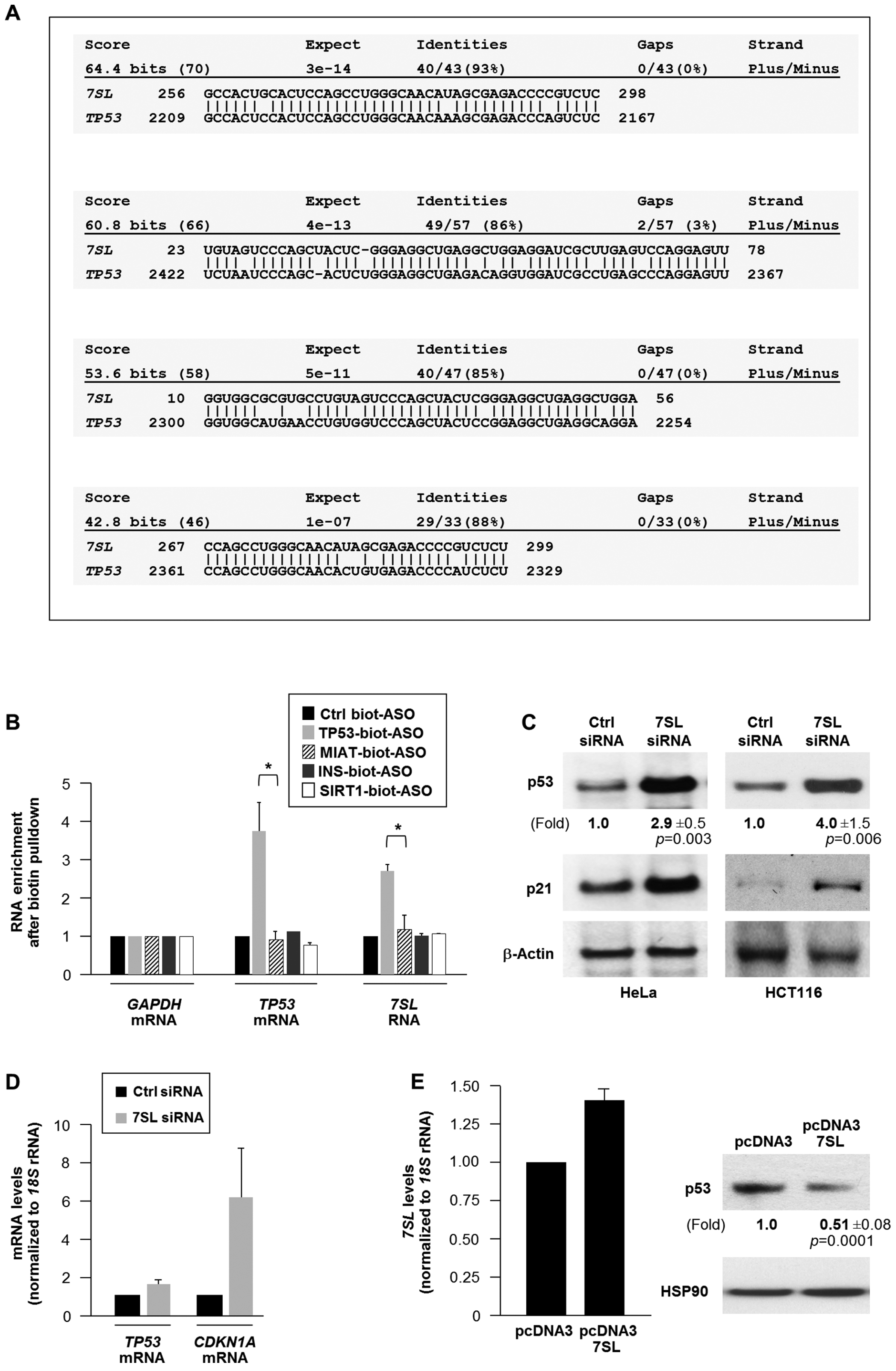

```
Score                   Expect     Identities           Gaps         Strand
64.4 bits (70)          3e-14      40/43(93%)           0/43(0%)     Plus/Minus
7SL      256   GCCACUGCACUCCAGCCUGGGCAACAUAGCGAGACCCCGUCUC  298
               |||||| ||||||||||||||||||| |||||||||| |||||
TP53    2209   GCCACUCCACUCCAGCCUGGGCAACAAAGCGAGACCCAGUCUC  2167


Score                   Expect     Identities           Gaps         Strand
60.8 bits (66)          4e-13       49/57 (86%)         2/57 (3%)    Plus/Minus
7SL       23   UGUAGUCCCAGCUACUC-GGGAGGCUGAGGCUGGAGGAUCGCUUGAGUCCAGGAGUU  78
               |||| ||||||| |||| ||||||||||| | || ||||||| |||| |||||||||
TP53    2422   UCUAAUCCCAGC-ACUCUGGGAGGCUGAGACAGGUGGAUCGCCUGAGCCCAGGAGUU  2367


Score                   Expect     Identities           Gaps         Strand
53.6 bits (58)          5e-11      40/47(85%)           0/47(0%)     Plus/Minus
7SL       10   GGUGGCGCGUGCCUGUAGUCCCAGCUACUCGGGAGGCUGAGGCUGGA  56
               ||||||  |  ||||| ||||||||||||| |||||||||||| |||
TP53    2300   GGUGGCAUGAACCUGUGGUCCCAGCUACUCCGGAGGCUGAGGCAGGA  2254


Score                   Expect     Identities           Gaps         Strand
42.8 bits (46)          1e-07      29/33(88%)           0/33(0%)     Plus/Minus
7SL      267   CCAGCCUGGGCAACAUAGCGAGACCCCGUCUCU  299
               |||||||||||||||  | |||||||| |||||
TP53    2361   CCAGCCUGGGCAACACUGUGAGACCCCAUCUCU  2329
```

Figure 2. *7SL* binds *TP53* mRNA and lowers p53 abundance. (**A**) Sequence alignment of *7SL* and *TP53* mRNA using BLAST shows potential sense–antisense interactions. (**B**) *TP53* mRNA pulldown using the biotin-ASOs shown (see the Materials and Methods section) was followed by RT-qPCR analysis to quantify *TP53* mRNA and *7SL* levels; *GAPDH* mRNA was used for normalization. (**C**) HeLa cells were transfected with the indicated siRNAs; 48 h later, the levels of p53, p21 and loading control β-actin were assessed by western blot analysis. (**D**) The levels of *TP53* and *CDKN1A* mRNA (encoding p21) and normalization control *18S* rRNA were quantified by RT-qPCR. (**E**) Forty-eight hours after transfecting plasmids pcDNA3 or pcDNA3-7SL, total cellular *7SL* levels were measured by RT-qPCR analysis (left) and the levels of p53 and loading control HSP90 by western blot analysis (right). Data in (B) and (E) are the means + S.D. from three independent experiments. In (C) and (E), the means ± standard deviation of p53 signals are indicated and the *p* values are shown.

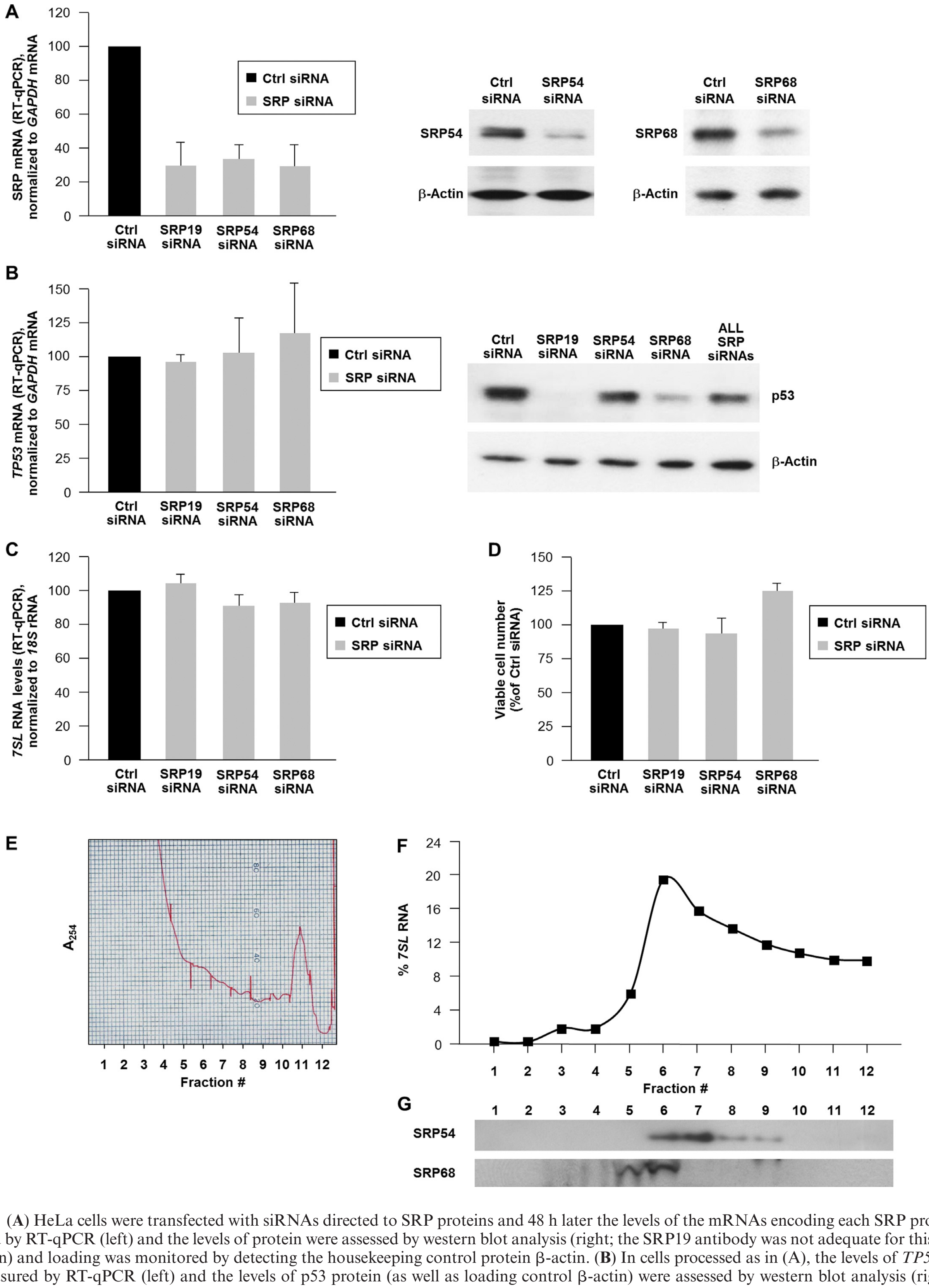

Figure 3. (**A**) HeLa cells were transfected with siRNAs directed to SRP proteins and 48 h later the levels of the mRNAs encoding each SRP protein were measured by RT-qPCR (left) and the levels of protein were assessed by western blot analysis (right; the SRP19 antibody was not adequate for this analysis, not shown) and loading was monitored by detecting the housekeeping control protein β-actin. (**B**) In cells processed as in (A), the levels of *TP53* mRNA were measured by RT-qPCR (left) and the levels of p53 protein (as well as loading control β-actin) were assessed by western blot analysis (right). This group included analysis of cells in which SRP68, SRP54 and SRP19 were silenced simultaneously ('ALL SRP siRNAs'). (**C**) In cells processed as in (A), the levels of *7SL* were measured by RT-qPCR analysis. (**D**) Forty-eight hours after transfection as in (A), cells were counted using a hemocytometer. In (A)–(D), data are shown as the means + S.D. from three independent experiments. (**E**)–(**G**) From each of 12 fractions from glycerol gradients shown in the global RNA profile (10-40% glycerol) (E), RNA was isolated and used for RT-qPCR analysis of *7SL* levels (**F**), and protein was precipitated and used for western blot analysis of SRP54 and SRP68. Data are representative of three independent experiments.

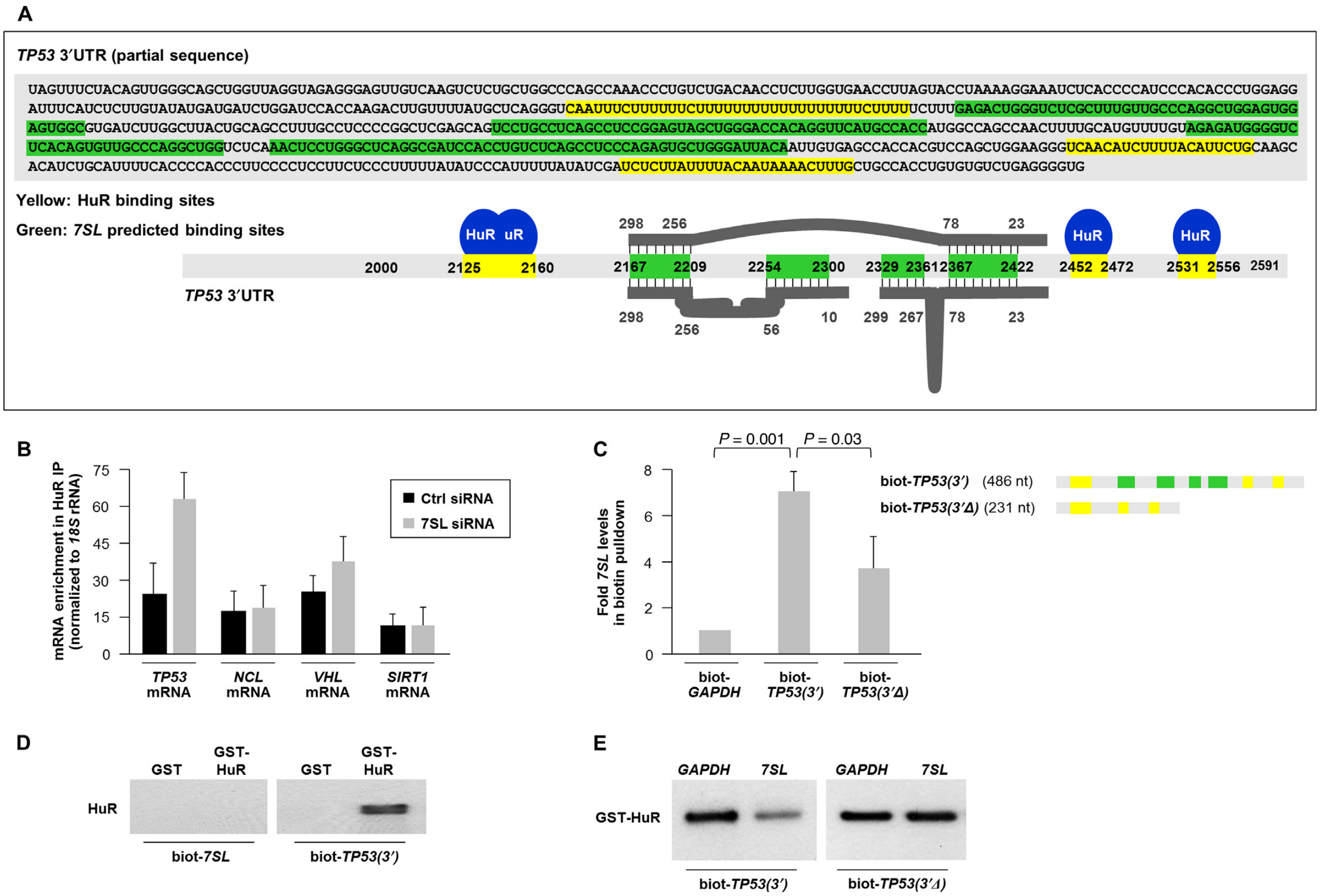

Figure 4. Competitive regulation of p53 expression by *7SL* and HuR. (**A**) Schematic of *TP53* mRNA depicting potential binding sites for *7SL* (green) and HuR (yellow). The thick grey lines and numbers above and below *TP53* 3′UTR depict regions of complementarity with *7SL*. (**B**) HeLa cells were transfected with 7SL siRNA; 48 h later, HuR association with the indicated mRNAs was quantified by RIP analysis. Data were normalized to the levels of *GAPDH* mRNA in each IP sample and represented as the enrichment of each mRNA relative to the levels in IgG IP. (**C**) Top, partial *in vitro TP53* 3′UTR biotinylated transcripts bearing the sites of interaction with HuR and *7SL* [biot-TP53(3′)] or bearing only the sites of interaction with HuR [biot-TP53(3′Δ)]. Bottom, biotinylated RNAs were incubated with non-biotinylated *7SL* and the levels of *7SL* in the pulldown were measured by RT-qPCR analysis. (**D**) GST or GST-HuR were incubated *in vitro* with the biotinylated RNAs shown; following pulldown, western blot analysis was carried out to detect HuR levels. (**E**) GST-HuR was incubated *in vitro* with the biotinylated and non-biotinylated RNAs shown and its presence in the pulldown material was assessed by western blot analysis. Data in (B) are the means + S.D. from three independent experiments; data in (C) and (E) are average of two repeats showing similar results; data in (D) are representative of three repeats.

Antagonistic effects of *7SL* and HuR on p53 translation

Consistent with earlier evidence (23), HuR promoted p53 expression (Figure 5A), but the enhancement of p53 levels after silencing *7SL* was inhibited when HuR was silenced (Figure 5A). These data suggested that HuR and *7SL* competed for binding to *TP53* mRNA and that HuR was required for enhancing p53 expression in *7SL*-silenced cells. Since modulating *7SL* or HuR did not alter *TP53* mRNA levels [Figure 2D; (23)], we hypothesized that *7SL* RNA and HuR may regulate *p53* mRNA translation by binding to the *TP53* 3′UTR. To test this hypothesis, we cloned the *TP53* 3′UTR [nucleotides 1421–2629 (23)] into a dual luciferase construct [pmirGlo-p53(3′UTR)] and prepared a *TP53* 3′UTR reporter plasmid lacking the *7SL* interaction region (nucleotides 2161–2300) [pmirGlo-p53(3′UTRΔ). In cells transfected with pmirGlo-p53(3′UTR), luciferase activity [FL/RL] increased in *7SL*-silenced cells and decreased in HuR-silenced cells (Figure 5B). Importantly, the induction in luciferase activity by *7SL* silencing was attenuated in cells with both *7SL* and HuR silenced and in cells expressing pmirGlo-p53(3′UTRΔ). Moreover, HuR binding to *TP53* 3′UTR, as determined by ribonucleoprotein immunoprecipitation (RIP) analysis of HuR binding to *FL* RNA expressed from the reporter plasmids in Figure 5B, revealed that removing the *7SL* site increased the interaction of HuR with the *TP53* 3′UTR. Since the precise *TP53* 3′UTR nucleotides within the HuR PAR-CLIP sites with which HuR interacts are not known, we were unable to test the impact of introducing point mutations upon *7SL* binding to *TP53* 3′UTR. Collectively, these results indicate that *7SL* repressed reporter activity by interacting with the *TP53* 3′UTR region complementary to *7SL* and that derepression by silencing *7SL* required the presence of HuR.

To study if these effects were also observed with the endogenous *TP53* mRNA, we performed two sets of experiments. First, nascent p53 translation was measured by a brief (15 min long) incubation of HeLa cells with L-

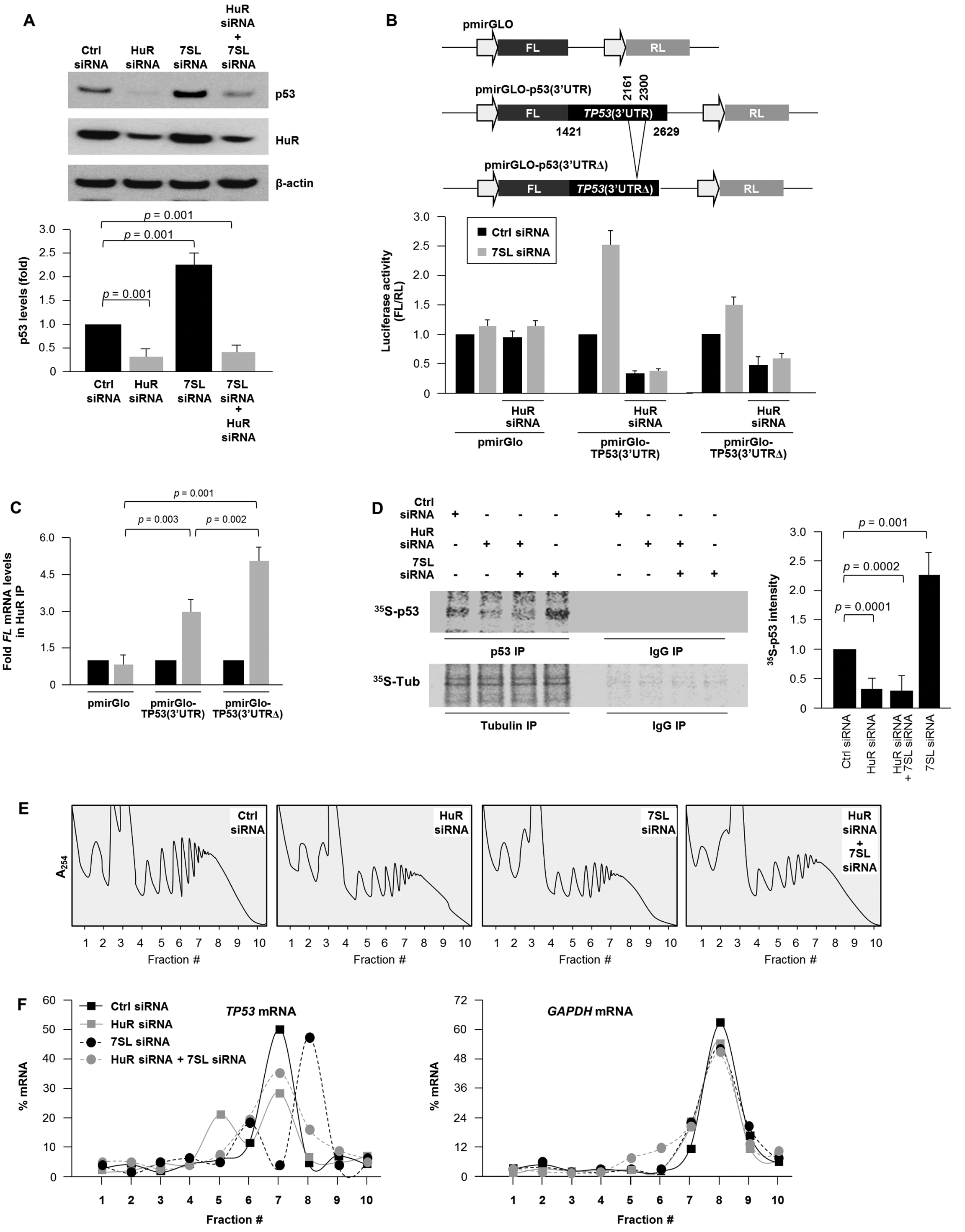

Figure 5. Opposite regulation of p53 translation by *7SL* and HuR. (**A**) HeLa cells were transfected with the indicated siRNAs; 48 h later, the levels of p53, HuR and loading control β-actin were assessed by western blot analysis and p53 signals were quantified by densitometry and plotted. (**B**) Top, luciferase reporter constructs pmirGLO-p53(3′UTR), bearing partial sequence of *TP53* 3′UTR (nucleotides 1421–2629) that includes *7SL* and HuR binding sites, and pmirGLO-p53(3′UTRΔ) that lacks the *7SL* interaction site (nucleotides 2161–2300). Thirty-six hours after transfection of the indicated siRNAs, luciferase plasmids were transfected for 6 h and followed by luciferase assay 12 h thereafter. (**C**) RIP analysis of HuR interaction with the *FL* mRNAs expressed from the reporters in panel (B); data represent enrichment levels relative to *FL* mRNA abundance in IgG IP, using *GAPDH* mRNA for normalization. (**D**) *De novo* translation of p53 as well as housekeeping control protein β-Tubulin (Tub), as assessed by ^{35}S-p53 IP and ^{35}S-Tub IP 48 h after transfection of the indicated siRNAs (details in Materials and Methods section); 'Fold' quantified ^{35}S-p53 signals, relative to signals in the Ctrl siRNA group. (**E**) and (**F**) Cells were transfected as described in (A) followed by fractionation through sucrose gradients. Global RNA profile for these transfection conditions are shown (E). The relative distribution of *TP53* mRNA (and housekeeping *GAPDH* mRNA) was studied by RT-qPCR analysis of RNA in each of 10 gradient fractions (F). Data in (A)–(C) represent the means and S.D. from three independent experiments; data in (D)–(F) are representative of three independent experiments; *P* values are shown.

[^{35}S]methionine and L-[^{35}S]cysteine, after which p53 and housekeeping control protein β-Tubulin (β-Tub) were subjected to IP and the incorporation of radiolabeled amino acids visualized by autoradiography; this assay routinely yields faint signals because the time of incorporation of radiolabeled amino acids is very brief (15 min) to ensure that the signal reflects only *de novo* translation. As shown, relative to control cells, *de novo* p53 translation was lower in HuR siRNA-transfected cells and was higher in 7SL siRNA-transfected cells (Figure 5D). Consistent with the pattern of luciferase activity (Figure 5B), the *7SL* silencing-induced p53 translation was lost in cells in which *7SL* and HuR were silenced (Figure 5D).

Second, we investigated whether the levels of *7SL* and HuR affected p53 translation by monitoring the association of *TP53* mRNA with the translational machinery in each of the four transfection groups. Cytoplasmic extracts were fractionated on sucrose gradients and the relative abundance of *TP53* mRNA in each fraction was calculated to measure the association of *TP53* mRNA with the translational apparatus. As shown in Figure 5E, *TP53* mRNA levels were very low in non-translating and low-translating fractions of the gradient (fractions 1–6). In control cells, *TP53* mRNA was found in the actively translating fractions of the gradient (fractions 7–9); in this section of the gradient, *TP53* mRNA in *7SL*-silenced cells showed a rightward shift, indicating that *TP53* mRNA associated with larger polysomes and further suggesting that *7SL* suppressed the initiation of *TP53* mRNA translation (Figure 5F). By contrast, in HuR-silenced cells, the peak of *TP53* mRNA decreased compared to the peak in control cells, even after silencing *7SL*, indicating that a smaller number of *TP53* mRNAs were engaged in translation (Figure 5F). These differences were not seen when testing the distribution of a control transcript (*GAPDH* mRNA) that encodes the housekeeping protein GAPDH in the four groups (Figure 5F). In summary, these data indicated that *7SL* suppresses *TP53* mRNA translation while HuR is required for efficient translation even in the absence of *7SL* RNA.

7SL deficiency promotes cell cycle arrest, senescence and autophagy

Several studies underscore the role of HuR in orchestrating anti-apoptotic and pro-survival programs (13,27). In agreement with this influence, HuR silencing decreased cell numbers and silencing both HuR and *7SL* decreased cell numbers even further (Supplementary Figure S4A). Therefore, we sought to study in more detail the cellular response to lowering *7SL* levels. The *7SL* silencing-triggered decrease in cell numbers was specifically dependent on p53, since p53-deficient (p53KO) HCT116 cells were refractory to the loss in cell number after silencing *7SL* (Supplementary Figure S4B and C). These data indicated that silencing *7SL* caused growth arrest at least in part by inducing p53 levels. Thus, we investigated other p53-regulated cellular processes—cell cycle, senescence and autophagy. By fluorescence-activated cell sorting (FACS) analysis, silencing *7SL* led to an increase in the G1 and G2 compartments and a decrease in S-phase cells (Figure 6A). *7SL* silencing also lowered [^{3}H]-thymidine incorporation (Figure 6B), further indicating that silencing *7SL* inhibited DNA replication, which occurs during S phase; conversely, overexpressing *7SL* as explained in Figure 2E increased [^{3}H]-thymidine incorporation (Supplementary Figure S4E).

In keeping with the growth suppression that characterizes senescence, 5 days after silencing *7SL*, HeLa cells displayed high activity of the senescence marker SA-β-gal (senescence-associated-β-galactosidase; Figure 6C). Finally, we assessed the effect of *7SL* on autophagy, another process influenced by p53 (28). Western blot analysis of the processed form of the microtubule-associated protein 1 light chain 3 (LC3)-II, broadly used to monitor autophagy because it correlates with the number of autophagosomes (29), showed that silencing *7SL* selectively elevated LC3-II (Figure 6D). Moreover, silencing *7SL* in cells transfected with plasmid pGFP-LC3, which expresses green fluorescent protein (GFP)-tagged LC3, revealed a pattern of distinct GFP-LC3 puncta staining that is characteristic of the presence of autophagosomes (30) (Figure 6E). Together, these data indicate that *7SL* silencing reduced cell proliferation and promoted cellular senescence and autophagy, and lend support to the notion that suppression of p53 by *7SL* promotes cell growth.

DISCUSSION

Given that the ncRNA *7SL* is more abundant in cancer tissues compared to normal tissues and is required for cancer cell growth [(21,22), Figure 1], we have studied the possibility that *7SL* promotes cancer cell growth by lowering the expression of the tumor suppressor p53. We identified an RNA-dependent interaction between *7SL* and *TP53* 3′UTR (Figures 2 and 4) that prevents HuR binding to *TP53* mRNA and thereby suppresses p53 translation (Figure 5); these effects by *7SL* appeared to be independent of its function as a component of the SRP (Figure 3). We postulate that by lowering p53 expression levels, *7SL* promotes cell cycle progression and suppresses cellular senescence and autophagy, all of which are key phenotypes of cancer cells (Figure 6).

ncRNAs bind and regulate the fate of target mRNAs by forming complexes that usually contain RBPs. The consequences of these lncRNA–mRNA interactions vary widely. For instance, *1/2-sbsRNAs* lncRNAs enhance target mRNA decay (3), while *BACE1AS* prevents the degradation of its target transcript, *BACE1* mRNA (4). The AS *Uchl1* lncRNA interacts with *Uchl1* mRNA to enhance its translation (6), while *lincRNA-p21* represses the translation of *JUNB* and *CTNNB* mRNAs (7). Similarly, we found that *7SL* interacts with *TP53* mRNA and repressed its translation. Our findings support growing evidence that lncRNA–mRNA interactions are a common mechanism to regulate mRNA fate and that RBPs are functionally involved. For instance, the repressive influence of *lincRNA-p21* upon *JUNB* and *CTNNB* mRNAs required the actions of Rck and Fmrp (7). In cells and *in vitro*, HuR binding to *TP53* mRNA was restricted by the abundance of *7SL*, indicating a competitive interaction between HuR and *7SL* (Figure 4). A similar competition between HuR and miR-494 was previously reported to regulate *NCL* mRNA translation (18). However, the present study constitutes the first example, to

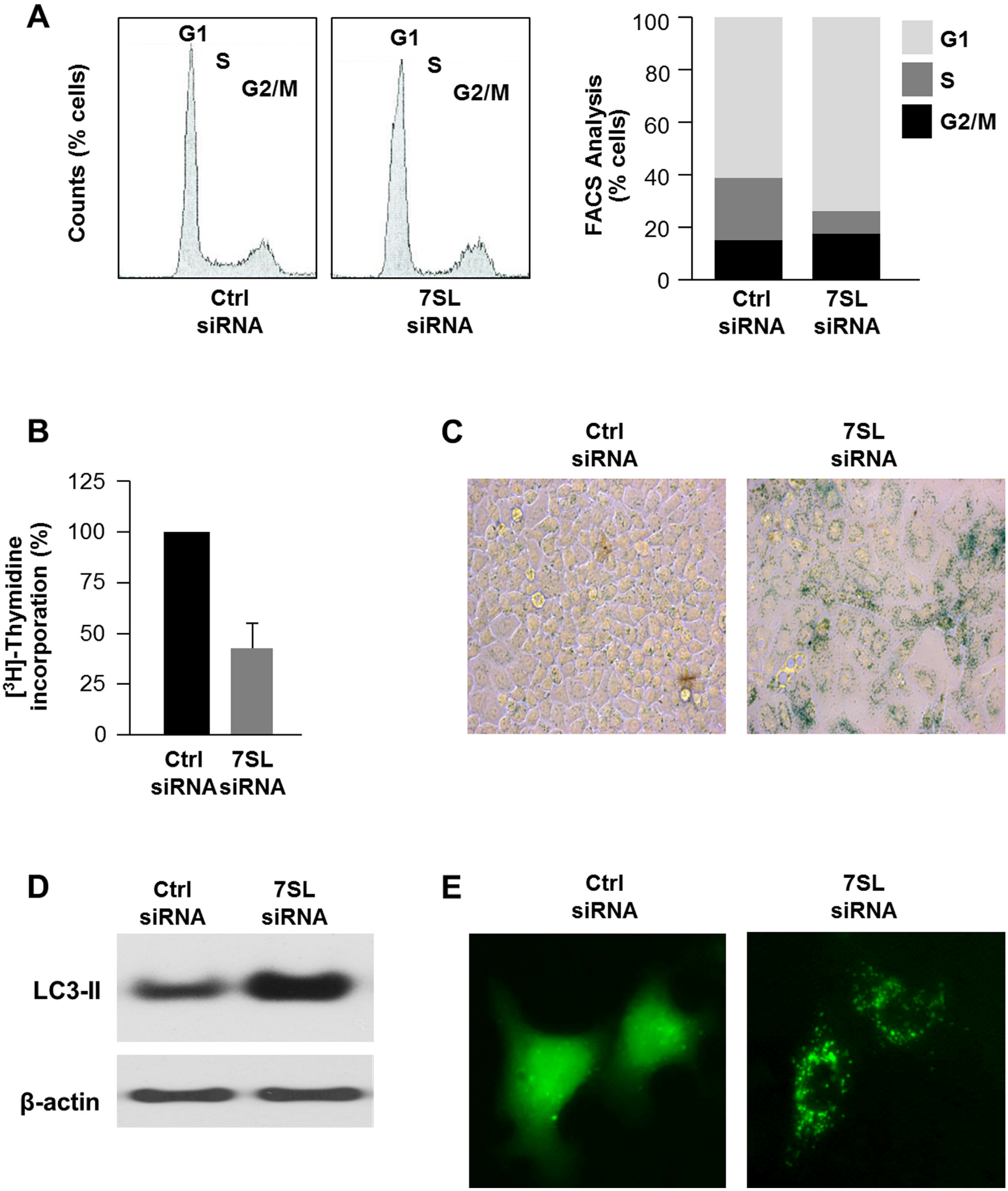

Figure 6. Influence of *7SL* silencing on cell phenotype. (**A**) Forty-eight hours after transfection of HeLa cells with Ctrl siRNA or 7SL siRNA, cells were subjected to FACS analysis (left) and the relative G1, S and G2/M compartments calculated (right). Data are representative of three independent experiments. (**B**) Measurement of [^{3}H]-thymidine incorporation by 48 h after transfection of HeLa cells with Ctrl siRNA or *7SL* siRNA. (**C**) β-galactosidase activity in HeLa cells 5 days after transfection with either Ctrl siRNA or *7SL* siRNA. (**D**) Western blot analysis of the autophagy marker LC3 in 48 h after transfection of HeLa cells with Ctrl siRNA or 7SL siRNA. (**E**) HeLa cells were transfected with a plasmid that expresses GFP-LC3 (a fluorescent fusion protein that is recruited to autophagosomes) and with either Ctrl siRNA or *7SL* siRNA; 48 h later, GFP-LC3 signals were visualized by fluorescence microscopy.

our knowledge, of a long ncRNA that competes with an RBP to regulate the post-transcriptional outcome (translation in this case) of a shared target mRNA.

The expression of p53 is also regulated by other lncRNAs, including *H19*, maternally expressed gene 3 (*MEG3*) and *lincRNA-RoR* (31). *H19*, essential for human tumor growth, was found to interact with p53 and suppressed p53 function post-translationally (32,33). In contrast, *MEG3*, a tumor suppressor lncRNA, regulates the transcriptional activation of p53 by reducing the levels of MDM2 (mouse double minute 2 homolog) (34), which mediates p53 degradation. However, tumor suppression by *MEG3* was found to be both p53-dependent and p53-independent (35). In this study, we found that the effect of *7SL* silencing on HeLa cell growth is largely p53-dependent, since p53-deficient HCT116 cells were refractory to *7SL* silencing (Supplementary Figure S4B and C). Recently, *lincRNA-RoR*, which is transcriptionally induced by p53, was found to repress p53 translation indirectly by interacting with hnRNP I (36). These findings and our study indicate the existence of more complex regulatory levels of *TP53* mRNA and p53 protein by lncRNAs. Additionally, p53 translation is positively regulated via the formation of a partial hybrid between the *TP53* 5′UTR and 3′UTR (37). Whether this intramolecular interaction is functionally linked to the effects of *7SL* or HuR is the subject of ongoing studies.

The discovery that lowering *7SL* RNA results in growth arrest raises the possibility that *7SL* could enhance the growth of malignant cells. These actions could be mediated by p53 in large part, as p53 potently regulates several cellular processes involved in tumorigenesis, such as cell survival, proliferation, senescence and autophagy (38). Silencing *7SL* recapitulated the inhibition of cancer cell growth in models of therapy-induced senescence in which p53 expression is elevated (39). Similarly, the discovery that *7SL* is more abundant in cancer tissues suggests that *7SL* is required for cancer cell growth and might have oncogenic effects [Figure 1 (21,22)]. Whether *7SL* also influences the expression of other proteins involved in proliferation of cancer cells remains to be investigated. An interesting finding of our study is that *7SL* silencing-induced cell cycle arrest and senescence occur despite sustained levels of HuR (Figure 6). This finding indicates that high p53 levels force cell cycle arrest and senescence, while HuR can help maintain cell survival, as more cell death is observed in HuR-silenced cells together with *7SL* RNA silencing (Supplementary Figure S4A). Although HuR is more abundant in cancer cells (40), p53 levels are usually low in cancer. In light of the high levels of *7SL*, HuR may not be able to enhance *TP53* mRNA translation in cancer cells if *7SL* is elevated and outcompetes HuR. However, the stoichiometry of this competitive interaction awaits further study.

It is worth noting that in 1991, Sakamoto *et al.* (41) cloned and studied a 510-bp genomic fragment that contained 180 bp upstream and 30 bp downstream from the *7SL* sequence. The authors observed that transfection of HeLa cells with this vector suppressed cell proliferation and elevated *7SL* levels transiently (by 6 h after transfection). They proposed that the elevated presence of the 510-bp sequence, which contained binding sites for RNA Polymerase III, might ‘sponge’ RNA Pol III and alter its basal activity. In agreement with this possibility, the effect of overexpressing the 510-bp genomic *7SL* fragment was abolished by mutation of the Pol III binding site (41).

In light of the influence of *7SL* on p53 abundance, future work is warranted to test if *7SL* is broadly elevated in cancer cells and if the concentration of *7SL* is inversely correlated with that of p53. To test if *7SL* is oncogenic, studies are underway to examine if *7SL* promotes tumorigenesis in mice and whether such influence is linked to HuR levels. In sum, we have found that by influencing p53 levels, *7SL* and HuR affect gene expression programs modulated by p53. In the immediate future, studies are warranted to investigate if *7SL* is a valuable target of therapeutic intervention.

SUPPLEMENTARY DATA

Supplementary Data are available at NAR Online.

ACKNOWLEDGMENT

We thank R.P. Wersto (NIA, NIH) for assistance with FACS analysis.

FUNDING

National Institute on Aging-Intramural Research Program [NIA-IRP], National Institutes of Health [NIH].

Conflict of interest statement. None declared.

REFERENCES

1. Ulitsky,I. and Bartel,D.P. (2013) lincRNAs: genomics, evolution, and mechanisms. *Cell*, **154**, 26–46.
2. Yoon,J.H., Abdelmohsen,K. and Gorospe,M. (2013) Posttranscriptional gene regulation by long noncoding RNA. *J. Mol. Biol.*, **425**, 3723–3730.
3. Gong,C. and Maquat,L.E. (2011) lncRNAs transactivate STAU1-mediated mRNA decay by duplexing with 3′ UTRs via Alu elements. *Nature*, **470**, 284–288.
4. Faghihi,M.A., Modarresi,F., Khalil,A.M., Wood,D.E., Sahagan,B.G., Morgan,T.E., Finch,C.E., St Laurent,G. 3rd, Kenny,P.J. and Wahlestedt,C. (2008) Expression of a noncoding RNA is elevated in Alzheimer’s disease and drives rapid feed-forward regulation of beta-secretase. *Nat. Med.*, **14**, 723–730.
5. Faghihi,M.A., Zhang,M., Huang,J., Modarresi,F., Van der Brug,M.P., Nalls,M.A., Cookson,M.R., St-Laurent,G 3rd and Wahlestedt,C. (2010) Evidence for natural antisense transcript-mediated inhibition of microRNA function. *Genome Biol.*, **11**, R56.
6. Carrieri,C., Cimatti,L., Biagioli,M., Beugnet,A., Zucchelli,S., Fedele,S., Pesce,E., Ferrer,I., Collavin,L., Santoro,C. *et al.* (2012) Long non-coding antisense RNA controls Uchl1 translation through an embedded SINEB2 repeat. *Nature*, **491**, 454–457.
7. Yoon,J.H., Abdelmohsen,K., Srikantan,S., Yang,X., Martindale,J.L., De,S., Huarte,M., Zhan,M., Becker,K.G. and Gorospe,M. (2012) LincRNA-p21 suppresses target mRNA translation. *Mol. Cell*, **47**, 648–655.
8. Wilkie,G.S., Dickson,K.S. and Gray,N.K. (2003) Regulation of mRNA translation by 5′- and 3′-UTR-binding factors. *Trends Biochem. Sci.*, **28**, 182–188.
9. Wilusz,C.J. and Wilusz,J. (2004) Bringing the role of mRNA decay in the control of gene expression into focus. *Trends Genet.*, **20**, 491–497.
10. Glisovic,T., Bachorik,J.L., Yong,J. and Dreyfuss,G. (2008) RNA-binding proteins and post-transcriptional gene regulation. *FEBS Lett.* **582**, 1977–1986.
11. Mukherjee,N., Corcoran,D.L., Nusbaum,J.D., Reid,D.W., Georgiev,S., Hafner,M., Ascano,M. Jr, Tuschl,T., Ohler,U. and Keene,J.D. (2011) Integrative regulatory mapping indicates that the

RNA-binding protein HuR couples Pre-mRNA processing and mRNA stability. *Mol. Cell*, **43**, 327–339.

12. Srikantan,S. and Gorospe,M. (2012) HuR function in disease. *Front. Biosci.*, **17**, 189–205.
13. Abdelmohsen,K. and Gorospe,M. (2010) Posttranscriptional regulation of cancer traits by HuR. *WIRES RNA*, **1**, 214–229.
14. Eberhardt,W., Doller,A. and Pfeilschifter,J. (2012) Regulation of the mRNA-binding protein HuR by posttranslational modification: spotlight on phosphorylation. *Curr. Protein Pept. Sci.*, **13**, 380–390.
15. Yoon,J.H., Abdelmohsen,K., Srikantan,S., Yang,X., Martindale,J.L. and Gorospe,M. (2014) Tyrosine phosphorylation of HuR by JAK3 triggers dissociation and degradation of HuR target mRNAs. *Nucleic Acids Res.*, **42**, 1196–1208.
16. Bhattacharyya,S.N., Habermacher,R., Martine,U., Closs,E.I. and Filipowicz,W. (2006) Relief of microRNA-mediated translational repression in human cells subjected to stress. *Cell* **125**, 1111–1124.
17. Lal,A., Mazan-Mamczarz,K., Kawai,T., Yang,X., Martindale,J.L. and Gorospe,M. (2004) Concurrent versus individual binding of HuR and AUF1 to common labile target mRNAs. *EMBO J.*, **23**, 3092–3102.
18. Tominaga,K., Srikantan,S., Lee,E.K., Subaran,S.S., Martindale,J.L., Abdelmohsen,K. and Gorospe,M. (2011) Competitive regulation of Nucleolin expression by HuR and miR-494. *Mol. Cell. Biol.*, **31**, 4219–4231.
19. Bernstein,H.D., Zopf,D., Freymann,D.M. and Walter,P. (1993) Functional substitution of the signal recognition particle 54-Kda subunit by its Escherichia-coli homolog. *Proc. Natl. Acad. Sci. U.S.A.*, **90**, 5229–5233.
20. Labuda,D. and Zietkiewicz,E. (1994) Evolution of secondary structure in the family of 7sl-like RNAs. *J. Mol. Evol.*, **39**, 506–518.
21. Chen,W., Bocker,W., Brosius,J. and Tiedge,H. (1997) Expression of neural BC200 RNA in human tumours. *J. Pathol.*, **183**, 345–351.
22. White,R.J. (2004) RNA polymerase III transcription and cancer. *Oncogene*, **23**, 3208–3216.
23. Mazan-Mamczarz,K., Galbán,S., López de Silanes,I., Martindale,J.L., Atasoy,U., Keene,J.D. and Gorospe,M. (2003) RNA-binding protein HuR enhances p53 translation in response to ultraviolet light irradiation. *Proc. Natl. Acad. Sci. U.S.A.*, **100**, 8354–8359.
24. Abdelmohsen,K., Srikantan,S., Kuwano,Y. and Gorospe,M. (2008) miR-519 reduces cell proliferation by lowering RNA-binding protein HuR levels. *Proc. Natl. Acad. Sci. U.S.A.*, **105**, 20297–20302.
25. Abdelmohsen,K., Pullmann,R. Jr, Lal,A., Kim,H.H., Galban,S., Yang,X., Blethrow,J.D., Walker,M., Shubert,J., Gillespie,D.A. *et al.* (2007) Phosphorylation of HuR by Chk2 regulates SIRT1 expression. *Mol. Cell*, **25**, 543–557.
26. El-Deiry,W.S., Tokino,T., Velculescu,V.E., Levy,D.B., Parsons,R., Trent,J.M., Lin,D., Mercer,W.E., Kinzler,K.W. and Vogelstein,B. (1993) WAF1, a potential mediator of p53 tumor suppression. *Cell*, **75**, 817–825.
27. Abdelmohsen,K., Lal,A., Kim,H.H. and Gorospe,M. (2007) Posttranscriptional orchestration of an anti-apoptotic program by HuR. *Cell Cycle*, **6**, 1288–1292.
28. Maiuri,M.C., Galluzzi,L., Morselli,E., Kepp,O., Malik,S.A. and Kroemer,G. (2010) Autophagy regulation by p53. *Curr. Opin. Cell. Biol.*, **22**, 181–185.
29. Mann,S.S. and Hammarback,J.A. (1994) Molecular characterization of light chain-3—a microtubule-binding subunit of Map1a and Map1b. *J. Biol. Chem.*, **269**, 11492–11497.
30. Kabeya,Y., Mizushima,N., Yamamoto,A., Oshitani-Okamoto,S., Ohsumi,Y. and Yoshimori,T. (2004) LC3, GABARAP and GATE16 localize to autophagosomal membrane depending on form-II formation. *J. Cell. Sci.*, **117**, 2805–2812.
31. Baldassarre,A. and Masotti,A. (2012) Long Non-Coding RNAs and p53 Regulation. *Int. J. Mol. Sci.*, **13**, 16708–16717.
32. Barsyte-Lovejoy,D., Lau,S.K., Boutros,P.C., Khosravi,F., Jurisica,I., Andrulis,I.L., Tsao,M.S. and Penn,L.Z. (2006) The c-Myc oncogene directly induces the H19 noncoding RNA by allele-specific binding to potentiate tumorigenesis. *Cancer Res.*, **66**, 5330–5337.
33. Yang,F., Bi,J., Xue,X., Zheng,L., Zhi,K., Hua,J. and Fang,G. (2012) Up-regulated long non-coding RNA H19 contributes to proliferation of gastric cancer cells. *FEBS J.*, **279**, 3159–3165.
34. Zhang,X., Zhou,Y., Mehta,K.R., Danila,D.C., Scolavino,S., Johnson,S.R. and Klibanski,A. (2003) A pituitary-derived MEG3 isoform functions as a growth suppressor in tumor cells. *J. Clin. Endocr. Metab.*, **88**, 5119–5126.
35. Zhou,Y., Zhong,Y., Wang,Y., Zhang,X., Batista,D.L., Gejman,R., Ansell,P.J., Zhao,J., Weng,C. and Klibanski,A. (2007) Activation of p53 by MEG3 non-coding RNA. *J. Biol. Chem.* **282**, 24731–24742.
36. Zhang,A., Zhou,N., Huang,J., Liu,Q., Fukuda,K., Ma,D., Lu,Z., Bai,C., Watabe,K. and Mo,Y.Y. (2013) The human long non-coding RNA-RoR is a p53 repressor in response to DNA damage. *Cell Res.*, **23**, 340–350.
37. Chen,J. and Kastan,M.B. (2010) 5′-3′-UTR interactions regulate p53 mRNA translation and provide a target for modulating p53 induction after DNA damage. *Genes Dev.*, **24**, 2146–2156.
38. Bieging,K.T. and Attardi,L.D. (2012) Deconstructing p53 transcriptional networks in tumor suppression. *Trends Cell Biol.*, **22**, 97–106.
39. Berns,A. (2002) Senescence: a companion in chemotherapy? *Cancer Cell*, **1**, 309–311.
40. Abdelmohsen,K., Kim,M.M., Srikantan,S., Mercken,E.M., Brennan,S.E., Wilson,G.M., de Cabo,R. and Gorospe,M. (2010) miR-519 suppresses tumor growth by reducing HuR levels. *Cell Cycle*, **9**, 1354–1359.
41. Sakamoto,K., Fordis,C.M., Corsico,C.D., Howard,T.H. and Howard,B.H. (1991) Modulation of HeLa cell growth by transfected 7SL RNA and Alu gene sequences. *J. Biol. Chem.* **266**, 3031–3038.